Pseudomonas fitomaticsae sp. nov., isolated at Marimurtra Botanical Garden in Blanes, Catalonia-Spain

Kostadin Evgeniev Atanasov[1,2], David Miñana Galbis[3], Deborah Cornadó[4], Annabel Serpico[4], Guiomar Sánchez[4], Montserrat Bosch[4], Albert Ferrer[1,5] and Teresa Altabella[1,2]

[1]Center for Research in Agricultural Genomics (CSIC-IRTA-UAB-UB), Bellaterra, Barcelona, Spain.

[2]Department of Biology, Healthcare and the Environment, Plant Physiology Section, Faculty of Pharmacy and Food Sciences, Universitat de Barcelona, Spain.

[3]Department of Biology, Healthcare and the Environment, Microbiology Section, Faculty of Pharmacy and Food Sciences, Universitat de Barcelona, Spain.

[4]Applied Microbiology and Biotechnology Unit, LEITAT Technological Center, Terrassa, Spain.

[5]Department of Biochemistry and Physiology, Faculty of Pharmacy and Food Sciences, Universitat de Barcelona, Spain.

Corresponding author: Kostadin E. Atanasov

The email address for the corresponding author: evgenievatanassov@ub.edu

Keywords: *Pseudomonas fitomaticsae* FIT81^T, multilocus sequence analysis, genome-to-genome comparison, genome assembly.

Repositories:

Bio Project: PRJNA705867; Bio Sample: SAMN19241968; SRR14663887; Assembly: CP075567; 16s rRNA sequence ID: MZ773500.1.

ABSTRACT

In the framework of the research project called FITOMATICS, we have isolated and characterized a bacterial plant-endophyte from the rhizomes of *Iris germanica*, hereafter referred to as strain FIT81^T. The bacterium is Gram negative, rod-shaped with lophotrichous flagella, and catalase and oxidase positive. The optimal growth temperature of strain FIT81^T is 28ºC, although it can grow within a temperature range of 4ºC to 32ºC. The pH growth tolerance ranges between 5 and 10, and it tolerates 4% (w/v) NaCl concentration. A 16S rRNA phylogenetic analysis positioned strain FIT81^T within the genus *Pseudomonas*, and multilocus sequence analysis (MLSA) revealed that *P. gozinkensis* IzPS32d^T, *P. glycinae* MS586^T, *P. allokribbensis* IzPS23^T, '*P. kribbensis*' 46-2, and *P. koreensis* PS9-14^T are the top five most closely related species, which were selected for further genome-to-genome comparisons, as well as for physiological and chemotaxonomical characterization. The genome size of strain FIT81^T is 6,492,796 base-pairs in length, with 60.6% of GC content. Average nucleotide identity (ANI) and digital DNA-DNA hybridization (dDDH) yielded values of 93.6% and 56.1%, respectively, when FIT81^T genome was compared to that of the closest type-species *P. gozinkensis* IzPS32d^T. Taken together, the obtained genomic, physiologic, and chemotaxonomic data indicate that strain FIT81^T is different from its closest relative species, which lead us to suggest that it is a novel species to be included in the list of type-strains with the name *Pseudomonas fitomaticsae* FIT81^T (=CECT 30374^T =DSM 112699^T).

INTRODUCTION

Land plants are soil-dependent organisms that have the capacity to interact with a plethora of multikingdom microorganisms. Among these are the so-called bacterial endophytes, which can enter and reside within the plant tissues without causing disease symptoms but, on the contrary, play a crucial role in promoting plant growth and defense by stimulating nutrient mobilization, synthesis of hormones and nutrients, and protection against biotic and abiotic stress [1, 2]. In addition to their recognized potential as plant-growth promoting organisms, endophytic bacteria have gained special interest because of their capacity to produce a broad range of bioactive metabolites, such as bactericides, antibiotics, fungicides, antivirals, and many others [3, 4].

One of the most frequently genus of endophytic bacterial is *Pseudomonas,* which is a ubiquitous Pseudomonadota, rod-shaped, aerobic, Gram negative and non-spore forming with high capacity to utilize diverse compounds as carbon source, colonize a broad range of eukaryotic host, and produce a wide array of specialized metabolites [5]. So far, a total of 299 *Pseudomonas* species with validly published and correct names are described for this genus (https://lpsn.dsmz.de/genus/pseudomonas).

Pseudomonas species classification was first performed by using traditional phenotypical characterization methods but, more recently, molecular techniques have emerged as key analytical tools to aim species delineation. At present, multilocus sequence analysis (MLSA) technique is used to study phylogenetic relationships among species. For instance, by using MLSA, Peix *et al.* [6] suggested the division of *Pseudomonas* in three lineages: *P. fluorescens*, *P. aeruginosa* and *P. pertucinogena*, from which *P. fluorescens* was also classified in seven different groups. On the other hand, Hesse *et al.* [7] compared the genomes of type and none-type strains, as well as of subspecies, and suggested the division of *Pseudomonas* in thirteen groups of species, being *P. fluorescens* the group containing the highest number of species,

which was then divided in ten subgroups. More recently, Rudra and Gupta [8] used 118 concatenated conserved protein codifying genes from 255 genomes and showed a distinct lineage for some halotolerant *Pseudomonas* species which were grouped in a Pertucinogena clade. In further analysis, the authors identified 24 conserved signature indels in diverse cellular functions proteins which supported the reclassification of *P. pertucinogena* to the new proposed genus *Halopseudomonas* were the type species is *Halopseudomonas pertucinogena*. In this work, we describe the characterization of a new *Pseudomonas* species candidate isolated from the rhizomes of *Iris germanica*, *Pseudomonas fitomaticsae*, in the framework of a research project (FITOMATICS) focused on the isolation and characterization of plant-endophytic microorganisms with the potential to produce secondary specialized metabolites.

ISOLATION AND ECOLOGY

For bacteria isolation, rhizomes of *Iris germanica* from the Marimurtra Botanical Garden of Blanes in Catalonia, Spain (41.67666º N; 2.80194 E) were used. Plants were examined for pests, lesions or any disease symptoms, and only healthy plants were selected. Rhizomes were collected *in situ*, maintaining plant integrity, and soil was detached manually from the rhizomes. Samples were washed with sterile distilled water and phosphate buffered saline solution (PBS) at pH 7.4, and surface sterilized essentially as reported by Kumar *et al*. [9]. The rhizomes were first soaked in 70% ethanol for 5 min and then in 2% sodium hypochlorite solution for 10 min, followed by 45 min in 70% ethanol. Finally, they were thoroughly washed with sterile distilled water to remove any remaining ethanol. Endophytic bacteria were released from the inner plant tissue by homogenizing the rhizomes in PBS. Then a two-fold serial dilution of the crude-extract was prepared, and 50 µl of each sample were spread on Tryptic Soy Agar medium (TSA, Sigma-Aldrich, St Louis, USA) plates, which were incubated at 30ºC for up to two weeks. As soon as colonies appeared, they were individually transferred to 3 ml of Tryptic Soy Broth (TSB, Becton Dickinson, Franklin Lakes, USA) medium and cultured

over-night at 30ºC with constant shaking at 190 rpm. After endophyte extraction, the rhizomes were incubated in TSA medium at 30ºC for up to three weeks, and no bacterial growth was observed, thus demonstrating the effectiveness of the sterilization procedure. For long-term strain preservation, 800 µl of an over-night culture were mixed with 200 µl of 80% sterile glycerol and stored at -80ºC.

PHYLOGENETIC ANALYSIS

For DNA extraction, 2 ml of strain FIT81^T over-night TSB culture was used. Cells were recovered by centrifugation at 11,000 g for 3 min and the genomic DNA was extracted with Wizard Genomic DNA Extraction Kit according to manufacturer´s instructions (Promega, Madison, USA). Thirty ng of the genomic DNA was used for the 16S rRNA gene PCR amplification with the universal primers 27F (5'-AGAGTTTGATCCTGGCTCAG-3') and 1492R (5'-GGTTACCTTGTTACGACTT-3') [10], and AccuPrime Pfx polymerase (2.5 units) (Thermo Fisher Scientific, Waltham, USA). The PCR program was as follows: DNA denaturalization at 95ºC for 5 min, 25 cycles of amplification including denaturalization at 95ºC for 15 s, annealing at 50ºC for 30 s, 2 min extension at 72ºC, and 10 min at 72ºC for complete synthesis of amplification product. The PCR product was analyzed by agarose gel electrophoresis, purified using PCR clean-up columns (Macherey-Nagel GmbH & Co. KG, Düren, Germany), and SANGER-sequenced using primers 27F or 1492R. The resulting partial sequences were assembled in a unique consensus sequence with the DNA Dragon software (SequentiX, Klein Raden, Germany), which was analyzed by nucleotide BLAST (blastn) alignment on the NCBI database (https://www.ncbi.nlm.nih.gov/) under the parameters of standard database, uncultured/environmental sample sequence exclusion, and search limited to type material. Blast results positioned strain FIT81^T within the genus *Pseudomonas* with 100% of sequence similarity to '*P. kribbensis*' 46-2, *P. glycinae* MS586^T and *P. saponiphila* DSM 9751^T. Next, the entire 16S rRNA sequence was extracted from the FIT81^T genome annotation,

and a species search on the EzBioCloud taxonomically united database [11] was performed. A total of 33 species were selected from the EzTaxon and 13 from the NCBI nucleotide blast. *H. pertucinogena* (homotypic synonym of *P. pertucinogena*) NBRC 14163^T (AB680571) was used as a rooting group. The 16S rRNA sequences were aligned by the MUSCL algorithm [12] and a phylogenetic tree was constructed by the Maximum Likelihood method based on the Jukes-Cantor mode with MEGA7 [13, 14]. This analysis outputted an unprecise tree-branch clustering of strain FIT81^T, showing 99.9% of sequence similarity to *P. gozinkensis* IzPS32d^T, '*P. kribbensis*' 46-2, and *P. glycinae* MS4586^T (Fig. S1; Table S1). Hence, by using 16S rRNA phylogeny, it was not possible to locate the newly isolated strain in any subgroup of the *P. fluorescens* group [7]. Thus, a MLSA was conducted to improve resolution on the strain phylogeny. Protein-coding housekeeping genes *rpoB*, *gyrB* and *rpoD* were extracted from the NCBI genome annotation, whereas for some species genomes were annotated by Patric 3.6.12 with the Rapid Annotation using Subsystems Technology algorithm (RAST) [15]. Sequences of the 16S rRNA, *rpoB*, *gyrB*, and *rpoD* genes were concatenated, aligned with MUSCL algorithm, and a new MLSA-based Maximum Likelihood tree constructed (Fig. 1). The overall sequences similarities of the FIT81^T concatenated housekeeping genes were as follows: 98.2% to *P. gozinkensis* IzPS32d^T and *P. glycinae* MS4586^T; 97.9% to '*P. kribbensis*' 46-2; 97.4% to *P. allokribbensis* IzPS23^T and 97.0% to the *P. koreensis* PS9-14^T (Table S2). These results further supported the view that strain FIT81^T is closely related to *P. glycinae* MS4586^T and *P. gozinkensis* IzPS32d^T and positioned strain FIT81^T as a new candidate of the *P. koreensis* subgroup of the *P. fluorescens* group with a clear clustering differentiation to other *P. jessenii* and *P. gessardii* subgroups. Thus, the selection of species for the whole genome-based species comparisons and the physiological and chemical characterization was based on these MLSA-based phylogenetic relationships.

GENOME FEATURES

Genomic DNA from strain FIT81^T was extracted as described above, treated with RNase A DNase free (Panreac AppliChem, Darmstadt, Germany), and deproteinized by chloroform-isoamyl alcohol treatment. The DNA was cleaned and concentrated by using Genomic DNA Clean & Concentrator-10 columns (Zymo Research, Irvin, USA), and whole genome sequencing was carried out by combining the Illumina Novaseq (2x150 bp) and PacBio RSII platforms. The resulting sequence data were combined to generate a hybrid genome assembly by using Unicycler software [16]. Genome size of FIT81^T is 6,492,796 base-pair length with 60.6% of GC content, which agrees with genome size and GC content of *Pseudomonas* species isolated from environmental samples [17]. Gene annotation was performed by NCBI Prokaryotic Genome Annotation Pipeline (PGAP) [18–20]. A total number of 5,742 protein-coding genes, 19 rRNA coding genes (7 genes coding for 5S rRNAs, 6 genes coding for 16S rRNAs and 6 genes coding for 23S rRNAs), and 72 tRNAs coding genes were predicted. Genome circularization was achieved by visualization of FIT81^T genome with Bandage software [21].

Furthermore, genome-to-genome computational comparisons were conducted between FIT81^T and the top five related species. The average nucleotide identity (ANI) and orthologous ANI (orthoANI) values obtained using the orthoANI Tool v0.93.1 [22] were, 93.6% and 94.2% to the *P. gozinkensis* IzPS32d^T; 93.6% and 94.0% to *P. glycinae* MS4586^T; 91.0% and 91.5% to *P. allokribbensis* IzPS23^T; 90.9% and 91.3% to '*P. kribbensis*' 46-2, 87.5% and 87.9% to the *P. koreensis* PS9-14^T, respectively. Usearch ANI analysis (ANIu) was performed with the ANI calculator web-based tool from the EzBioCloud [23] and ANI maximal unique matches (ANIm) estimated by JSpeciesWS [24]. The obtained ANIu and ANIm values were very similar to those from the orthoANI analysis. On the other hand, values obtained from the BLAST-based ANI (ANIb) calculated with JSpeciesWS were like the original ANI (Table 1).

Finally, we estimated the DNA-DNA hybridization (dDDH) values between species with the Genome-to-Genome Distance Calculator (GGDC) from the DSMZ webtool (https://ggdc-test.dsmz.de/ggdc.php#), with the BLAST+ local alignment algorithm using formula 2, which consists of the sum of all identities within high-scoring segment pairs (HSPs) divided per overall HSP length [25, 26]. Values from the dDDH were as follows: 56.1% [53.4 - 58.8%] to *P. gozinkensis* IzPS32d^T; 54.9% [52.1 - 57.6%] to *P. glycinae* MS4586^T; 44.4% [41.9 - 47.0%] to *P. allokribbensis* IzPS23^T; 43.9% [41.4 - 46.5%] to '*P. kribbensis*' 46-2; 34.7% [32.2 - 37.2%] to the *P. koreensis* PS9-14^T. All these genome-to-genome comparison percentages were below the threshold of 95-96% (ANI) and 70% (dDDH) for species boundaries delineation [27, 28], indicating there is enough nucleotide identity and dDDH differences to propose that strain FIT81^T is a different species from its closest relatives, which is further supported by the recently described methodology of bacteria and subspecies delineation proposed by Meier-Kolthoff on the Type (Strain) Genome Server (TYGS; https://tygs.dsmz.de) for prokaryote taxonomy [29]. FIT81^T genome was uploaded on the TYGS server and a total number of 14 out of 15,682 type strains available in the TYGS database passed the analysis as closest type strains. The position of FIT81^T in the phylogenetic tree constructed using the Genome Blast Distance Phylogeny (GBDP) calculator (Fig. 2) agreed with the MLSA phylogeny and the genome-to-genome comparison results.

GENOME MINING AND IDENTIFICATION OF ENDOPHYTIC LIFE-STYLE RELATED GENES

Genome assemblies of strains FIT81^T, *P. gozinkensis* IzPS32d^T, and *P. glycinae* MS4586^T were analyzed by using the Antibiotics and Secondary Metabolite Analysis Shell (antiSMASH) 6.0 webserver [30]. This computational analysis predicted the occurrence of 14 regions containing 10 putative biosynthetic gene clusters (BGCs) (Table S3). According to this, known cluster similarities were found for the cyclic lipopeptide lokisin (71%; *Pseudomonas* sp. [31]), the

194 oxidative stress protectant aryl polyene (APE) Vf or methyl (2E,4E,6E,8E,10E,12E)-13-(4-
195 hydroxy-3,5-dimethylphenyl)trideca-2,4,6,8,10,12-hexaenoate (40%; *Aliivibrio fischeri*
196 ES114 [32]), the detoxing compound rimosamide (20%; *Streptomyces rimosus* subsp. *rimosus*
197 ATCC 10970 [33]), the chromophoric siderophore pyoverdine (21%, 20%, and 11%;
198 *Pseudomonas protegens* Pf-5[34, 35]), the bioactive cyclic lipopeptide fengycin (13%;
199 *Bacillus velezensis* FZB42 [36, 37]), and the antibiotic lankacidin C (13%; [38–42]).
200 Interestingly a similar cluster prediction was obtained by antiSMASH among the three bacterial
201 species. Nevertheless, differences were found regarding the BGC for the nonribosomal
202 bioactive cyclic lipopeptide, bacillomycin D, which was predicted into the genome of *P.*
203 *glycinae* MS4586^T (20%; *B. velezensis* FZB42 [43]), but not in FIT81^T nor in *P. gozinkensis*
204 IzPS32d^T genomes. In addition, subtle differences exist concerning the BGC for the antifungal
205 compound fragin, which was detected in *P. gozinkensis* IzPS32d^T and *P. glycinae* MS4586^T
206 (37%; *Burkholderia cenocepacia* H111 [44]), but not in FIT81^T (Table S3). Genomic regions
207 containing BGCs were also annotated by using the Minimum Information about a Biosynthetic
208 Gene cluster (MIBiG [45]) repository, and the top three similarity score-based compounds
209 annotated (Table S3). To summarize, the genome mining analysis suggested a high
210 conservation of the lokisin BGC and variation some among species in the case of the BGCs for
211 bacillomycin D and fragin. The usefulness of those clusters as species and subspecies
212 identification markers could be further investigated.
213 During last decade, several genes have been suggested to serve as markers for the identification
214 of bacterial endophytes [46–51]. Thus, besides the genome mining, we performed a
215 computational search to identify endophytic-capacity life-style genes. This analysis revealed
216 that several endophyte gene markers potentially involved in phosphate solubilization, hormone
217 synthesis and response, metabolite transport, secretion and delivery systems, cell wall
218 attachment, plant polymer/modification, transcriptional regulators, siderophores, and

219 detoxification are present in the genomes of FIT81^T, *P. gozinkensis* IzPS32d^T, and *P. glycinae*
220 MS586^T (Table S4). Interestingly, a detoxification-related gene coding for acetaldehyde
221 dehydrogenase was found only in the genome of FIT81^T. These results together with the way
222 in which FIT81^T was isolated would confirm the endophytic nature of FIT81^T.

223 **PHYSIOLOGY AND CHEMOTAXONOMY**

224 Growth of strain FIT81^T is vigorous and forms white-mucoid colonies. The bacterium can grow
225 within a temperature range from 4ºC to 32ºC in TSA medium, being 28ºC the optimal growth
226 temperature. The pH growth tolerance in TSB medium was recorded within the range of pH5
227 to pH10, even though FIT81^T can resist alkaline conditions up to pH 12, at this pH growth is
228 seriously compromised. Limited growth capacity was observed at pH 4, and no growth was
229 observed at lower pH values after three weeks. Strain FIT81^T is a Gram-negative bacterium.
230 Uranyl acetate negative stain and transmission electron microscope (TEM) Bioscan Gatan,
231 JEM-1010 (JEOL) acquired image were used to visualize its lophotrichous flagella and to
232 measure the average cell size, which is 2±0.3 µm length and 0.8±0.2 µm width (N=10) (Fig.
233 3). Fluorescence production was observed when FIT81^T was cultured on solid King's B
234 medium (Duchefa Biochemie, Haarlem, TheNetherlands) at 28ºC and irradiated by 365 nm UV
235 light [52].

236 Polar lipids and fatty acids methyl esters (FAME) were determined by the Identification
237 Service, Leibniz - Institute DSMZ – Deutsche Sammlung von Mikroorganismen und
238 Zelkulturen GmbH (Braunschweig, Germany) from an over-night culture of FIT81^T in TSB
239 medium incubated at 28ºC with shaking at 190 rpm. Cells were pelleted by centrifugation at
240 4,000 g for 10 min at 4ºC, mixed with cryoprotectant ATCC Reagent-18
241 (https://www.atcc.org/resources/culture-guides/bacteriology-culture-guide), and freeze-dried
242 until further analysis. Cellular fatty acids from 30 mg of cells biomass were analyzed after
243 conversion into fatty acid methyl esters (FAMEs) by saponification, methylation and extraction

using minor modifications of the methods described by Miller [53] and Kuykendall *et al.* [54]. The FAME mixtures were then separated with gas chromatography and detected by a flame ionization detector using Sherlock Microbial Identification System (MIS) (MIDI, Microbial ID, Newark, DE 19711 U.S.A.). Peaks were automatically integrated, and fatty acid were identified and quantified by the MIS Standard Software (Microbial ID). Summed feature 3 was resolved by a GC-MS run on a Agilent GC-MS 7000D using an Agilent HP-5 ms UI 30 m x 250 µm x 0.25µm column, with a helium flow of 1.2 ml, with an injection of 1 µl with split ratio of 7.5:1. The oven program was as follows: initial temperature 170ºC, ramp 3ºC/min to 200°C, ramp 5°C/min to 270°C, ramp 120°C/min to 300°C and hold for 2 min. The inlet temperature was set to 170°C and then linearly increased with 200°C/min up to 350°C and hold for 5 min. The mass spectrometry parameters were set to aux temperature 230°C, source temperature 230°C, and electron impact ionization at 70 eV with mass range of m/z 40-600 or 40-800, respectively. Peaks were identified based on retention time and mass spectra. The position of single and double bounds was confirmed by derivatization to the corresponding dimethyl disulfide adducts [55]. Branched-chain fatty acid positions, cyclo-positions and multiple double bounds were determined by conversion to their 3-pyridylcarbinol and/or 4,4-dimethyloxazoline (DMOX) derivatives [56–58].

FIT81^T showed a *Pseudomonas* species typical profile $C_{10:0}$ 3-OH, $C_{12:0}$, and $C_{12:0}$ 3-OH fatty acids, which further supported its affiliation to genus *Pseudomonas* [59]. In addition, the major FAME was the unsaturated sixteen carbon aliphatic chain ($C_{16:0}$) with an average value of 30.6, which is slightly lower than those found in *P. gozinkensis* IzPS32d^T, *P. allokribbensis* IzPS23^T [20], '*P. kribbensis*' 46-2 [60], and *P. koreensis* PS9-14^T, but higher than those described for *P. glycinae* MS586^T [61]. Other fatty acids detected as FAMEs, were $C_{18:1}$ ω7c (14.4); $C_{12:0}$ 3-OH (4.4); $C_{10:0}$ 3-OH (4.1); $C_{12:0}$ 2-OH (3.9); $C_{17:0}$ cyclo (3.8); $C_{12:0}$ (3.7); $C_{18:0}$ (1.48), and traces of $C_{10:0}$, $C_{12:1}$ 3-OH, and $C_{14:0}$. Moreover, the summed feature 3 of $C_{16:1}$ ω7c/$C_{15:0}$ iso 2-

OH was clearly higher in FIT81^T than the levels found in *P. gozinkensis* IzPS32d^T [20], *P. glycinae* MS586^T [61], *P. allokribbensis* IzPS23^T [20], and '*P. kribbensis*' 46-2 [60] (Table 2). Polar lipids (PL) were extracted from 200 mg of freeze-dried cell material using a choroform:methanol:0.3% aqueous NaCl mixture and recovered into the chloroform phase [62]. PL were then separated by two-dimensional silica gel thin layer chromatography (TLC) by using chloroform:methanol:water and chloroform:methanol:acetic acid:water as mobile phase for first and second direction, respectively. Total lipid material was detected by using molybdatophosphoric, acid and specific functional groups were identified using spray reagents specific for defined functional groups [63]. The detected major compounds species were phosphatidylethanolamine (PE), diphosphatidylglycerol (DPG), phosphatidylglycerol (PG), glycolipid (GL), phospholipid (PL), and aminolipid (AL) (Fig. 4).

Carbon source utilization and chemical sensitivity was assessed with the miniaturized microplate assay of Biolog's GenIII (Biolog, Inc., Hayward, USA) following manufacturer´s instructions. The main differences between FIT81^T, *P. gozinkensis* IzPS32d^T, and *P. glycinae* MS586^T were found in the utilization of D-arabitol, D-serine, D-fructose-6-phosphate, D-galactose, pectin, D-fucose, inosine, D-galacturonic acid, L-galactonic acid lactone, glucuronamide, D-malic acid, bromo-succinic acid, α-keto-butyric acid, acetoacetic acid, and tween 40 (Table 3). FIT81^T exhibited chemical sensitivity to D-serine, guanidine HCl, lithium chloride, sodium butyrate, and sodium bromate, but it was tolerant to sodium lactate, fusidic acid, troleandomycin, rifamycin SV, minocycline, lincomycin, niaproof 4, vancomycin, tetrazolium violet, tetrazolium blue, nalidixic acid, potassium tellurite, and the monobactam aztreonam. FIT81^T shares high chemical compound tolerance with *P. gozinkensis* IzPS32d^T [23], but differences were found in the case of fusidic acid and minocycline. Enzyme activities of strain FIT81^T were analyzed on API 20 NE and API Zym strips (Biomerieux, Marcy-l'Étoile, France). The results obtained revealed that FIT81^T exhibits arginine dihydrolase, esculin

hydrolysis (β-glucosidase), and gelatin hydrolysis (protease) activities. It can also grow with N-acetyl-glucosamine while *P. gozinkensis* IzPS32d^T cannot. FIT81^T and *P. gozinkensis* IzPS32d^T have both C4 and C8 esterase lipase activity. Moreover, FIT81^T exhibited alkaline phosphatase, C14 lipase, trypsin, naphthol-AS-BI-phosphohydrolase, and acid phosphatase activities, which have not been described in *P. gozinkensis* IzPS32d^T. It is worth noting that acid phosphatase activity has been reported as a mechanism of phosphate solubilization from organic compounds, which further supports our claim that FIT81^T is an endophytic bacterium. Finally, the above biochemical comparisons among the five closest relative species to FIT81^T, as well as additional biochemical traits screened in API 20E and API 50CH, are summarized in more detail in Table 3.

In conclusion, the results from *de novo* genome sequencing, and the pangenome computational comparative analyses based on the top five phylogenetically-related species to strain FIT81^T, together with a thorough characterization of the bacterium chemo-physiological traits, leads to the claim that strain FIT81^T represents a novel *Pseudomonas* species.

DESCRIPTION OF *PSEUDOMONAS FITOMATICSAE* SP. NOV.

Pseudomonas fitomaticsae (fi.to.ma'tics.ae. N.L. gen. n. *fitomaticsae*, referring to the FITOMATICS research project), strain FIT81^T, isolated from the rhizomes of *Iris germanica* accessed at the Marimurtra Botanical Garden, from Blanes, Catalonia, Spain (41.67666º N; 2.80194 E).

The bacterium is Gram negative, rod-shaped with lophotrichous flagellum, and its average cell size is 2±0.3 µm length and 0.8±0.2 µm width. Its optimal growth temperature is 28ºC, forming white mucoid colonies in TSA medium, although it is also able to grow in a range of temperatures comprised between 4ºC and 32ºC. Growth was observed at pH values ranging from 5 to 10, with higher tolerance to alkaline pH than acidic one. The genome size is 6,492,796 base-pairs, with 60.6% GC content, and is predicted to harbor 5,742 protein-coding genes and

19 rRNA-coding genes. Among the latter, 7 genes are predicted to encode the 5S rRNA, 6 genes the 16S rRNA, and 6 genes the 23S rRNA. The type-strain of *P. fitomaticsae* FIT81^T was deposited at international recognized cell-type culture collection (FIT81^T =CECT 30374^T =DSM 112699^T) and is available for further biochemical, physiological, taxonomic, and genetic studies. Sequence Read Archive (SRA) was deposited at the National Center for Biotechnology Information (NCBI) database under the identification codes SRR14663887, PRJNA705867 (Bio Project), and SAMN19241968 (Bio Sample). 16S rRNA sequence was deposited in GenBank under the identification code MZ773500, and genome assembly was assigned the code CP075567.

Authors and contributors

Kostadin E. Atanasov (KA) designed experiments with the contribution of David Miñana-Galbis (DMG), Teresa Altabella (TA) and Albert Ferrer (AF). KA conducted experiments and analyzed data with contribution of DMG, TA, and AF. Deborah Cornadó (DC) isolated strain FIT81^T. Annabel Serpico (AS) participated in strain isolation and culturing. Guiomar Sánchez (GS) and Montserrat Bosch (MB) designed and supervised DC and AS work. This article was written by KA with contributions of all authors.

Conflicts of interest

Authors honestly declare that there are no economical, ethical, or publishing conflicts of interest.

Funding information

This work was funded by grants RTC-2017-6431 from FEDER/Ministerio de Ciencia, Innovación y Universidades-Agencia Estatal de Investigación (Spain), 2017SGR710 from the Generalitat de Catalunya, and by the CERCA Programme of the Generalitat de Catalunya. We also acknowledge financial support from the Spanish Ministerio de Economía y

343 Competitividad-Agencia Estatal de Investigación through the “Severo Ochoa Programme for
344 Centres of Excellence in R&D” SEV-2015- 0533 and CEX2019-000902-S.

345 **Acknowledgements**

346 We thank to Leigh A. Riley for help in genome annotation and submission at the NCBI
347 GenBank, Bethesda, Maryland USA. KA dedicates this manuscript in memory of Professor
348 Antonio Fernández Tiburcio from the Plant Physiology Section at the Faculty of Pharmacy and
349 Food Science of the Universitat de Barcelona.

350

References

1. **Kandel SL, Joubert PM, Doty SL.** Bacterial endophyte colonization and distribution within plants. Microorganisms 2017;5:77.

2. **Berg G, Köberl M, Rybakova D, Müller H, Grosch R, *et al*.** Plant microbial diversity is suggested as the key to future biocontrol and health trends. FEMS Microbiol Ecol 2017;93:10.1093/femsec/fix050.

3. **Gouda S, Das G, Sen SK, Shin HS, Patra JK.** Endophytes: A treasure house of bioactive compounds of medicinal importance. Front Microbiol 2016;7:1538.

4. **Hagaggi NSA, Mohamed AAA.** Plant-bacterial endophyte secondary metabolite matching: a case study. Arch Microbiol 2020;202:2679-2687.

5. **Rieusset L, Rey M, Muller D, Vacheron J, Gerin F, *et al*.** Secondary metabolites from plant-associated *Pseudomonas* are overproduced in biofilm. Microb Biotechnol 2020;13(5):1562-1580.

6. **Peix A, Ramírez-Bahena MH, Velázquez E.** The current status on the taxonomy of *Pseudomonas* revisited: An update. Infect Genet Evol 2018;57:106-116.

7. **Hesse C, Schulz F, Bull CT, Shaffer BT, Yan, *et al.*** Genome-based evolutionary history of *Pseudomonas* spp. Environ Microbiol 2018;20:2142-2159.

8. **Rudra B, Gupta RS.** Phylogenomic and comparative genomic analyses of species of the family *Pseudomonadaceae*: Proposals for the genera *Halopseudomonas* gen. nov. and *Atopomonas* gen. nov., merger of the genus *Oblitimonas* with the genus *Thiopseudomonas*, and transfer of some misclassified species of the genus *Pseudomonas* into other genera. Int J Syst Evol Microbiol. 2021;71:10.1099/ijsem.0.005011.

9. **Kumar A, Singh R, Yadav A, Giri DD, Singh PK, *et al.*** Isolation and characterization of bacterial endophytes of *Curcuma longa* L. 3 Biotech 2016;6:60.

10. **Miller CS, Handley KM, Wrighton KC, Frischkorn KR, Thomas BC, *et al.*** Short-read assembly of full-length 16S amplicons reveals bacterial diversity in subsurface sediments. PLoS One 2013;8:e56018

11. **Yoon SH, Ha SM, Kwon S, Lim J, Kim Y, *et al.*** Introducing EzBioCloud: A taxonomically united database of 16S rRNA gene sequences and whole-genome assemblies. Int J Syst Evol Microbiol 2017;67:1613-1617.

12. **Edgar RC.** MUSCLE: Multiple sequence alignment with high accuracy and high throughput. Nucleic Acids Res 2004;32:1792-1797.

13. **Kumar S, Stecher G, Tamura K.** MEGA7: Molecular evolutionary genetics analysis version 7.0 for bigger datasets. Mol Biol Evol 2016;33:1870-1874.

14. **Matsubara H, Yamanaka T (1969).** Evolution of protein molecules. In: Mammalian Protein Metabolism, pp. 21-132. Edited by Munro HN, Academic Press, New York.

15. **Brettin T, Davis JJ, Disz T, Edwards RA, Gerdes S, *et al*.** RASTtk: A modular and extensible implementation of the RAST algorithm for building custom annotation pipelines and annotating batches of genomes. Sci Rep 2015;5:8365.

16. **Wick RR, Judd LM, Gorrie CL, Holt KE.** Unicycler: Resolving bacterial genome assemblies from short and long sequencing reads. PLoS Comput Biol 2017;13:e1005595.

17. **Scales BS, Erb-Downward JR, Huffnagle IM, LiPuma JJ, Huffnagle GB.** Comparative genomics of *Pseudomonas fluorescens* subclade III strains from human lungs. BMC Genomics. 2015;16:1032.

18. **Haft DH, DiCuccio M, Badretdin A, *et al.*** RefSeq: An update on prokaryotic genome annotation and curation. Nucleic Acids Res.2018;46:D851-D860.

19. **Tatusova T, DiCuccio M, Badretdin A, Chetvernin V, Nawrocki EP, *et al.*** NCBI prokaryotic genome annotation pipeline. Nucleic Acids Res. 2016;44:6614-6624.

20. **Morimoto Y, Lu YJ, Zuo H, Aibibula Z, Tohya M, *et al.*** *Pseudomonas allokribbensis* sp. nov. and *Pseudomonas gozinkensis* sp. nov., Two new species isolated from a volcanic island, Izu Oshima, Japan. Curr Microbiol 2021;78:1670-1677.

21. **Wick RR, Schultz MB, Zobel J, Holt KE**. Bandage: interactive visualization of de novo genome assemblies. Bioinformatics. 2015;31:3350-3352.

22. **Lee I, Ouk Kim Y, Park SC, Chun J.** OrthoANI: An improved algorithm and software for calculating average nucleotide identity. Int J Syst Evol Microbiol 2016;66:1100-1103.

23. **Yoon SH, Ha SM, Lim J, Kwon S, Chun J.** A large-scale evaluation of algorithms to calculate average nucleotide identity. Antonie Van Leeuwenhoek 2017;110:1281-1286.

24. **Richter M, Rosselló-Móra R, Oliver Glöckner F, Peplies J.** JSpeciesWS: a web server for prokaryotic species circumscription based on pairwise genome comparison. Bioinformatics 2016;32:929-931.

25. **Meier-Kolthoff JP, Auch AF, Klenk HP, Göker M.** Genome sequence-based species delimitation with confidence intervals and improved distance functions. BMC Bioinformatics 2013;14:60.

26. **Auch AF, Klenk HP, Göker M.** Standard operating procedure for calculating genome-to-genome distances based on high-scoring segment pairs. Stand Genomic Sci 2010;2:142-148.

27. **Chun J, Oren A, Ventosa A, et al.** Proposed minimal standards for the use of genome data for the taxonomy of prokaryotes. Int J Syst Evol Microbiol 2018;68:461-466.

28. **Auch AF, von Jan M, Klenk HP, Göker M.** Digital DNA-DNA hybridization for microbial species delineation by means of genome-to-genome sequence comparison. Stand Genomic Sci 2010;2:117-134.

29. **Meier-Kolthoff JP, Göker M.** TYGS is an automated high-throughput platform for state-of-the-art genome-based taxonomy. Nat Commun 2019;10:2182.

30. **Blin K, Shaw S, Kloosterman AM, Charlop-Powers Z, van Wezel GP, *et al.*** antiSMASH 6.0: Improving cluster detection and comparison capabilities. Nucleic Acids Res 2021;49:W29-W35.

31. **Omoboye OO, Oni FE, Batool H, Yimer HZ, De Mot R, Höfte M.** *Pseudomonas* cyclic lipopeptides suppress the rice blast fungus *Magnaporthe oryzae* by Induced resistance and direct antagonism. Front Plant Sci 2019;10:901.

32. **Cimermancic P, Medema MH, Claesen J, Kurita K, Wieland Brown LC, *et al.*** Insights into secondary metabolism from a global analysis of prokaryotic biosynthetic gene clusters. Cell 2014;158:412-421.

33. **McClure RA, Goering AW, Ju KS, Baccile JA, Schroeder FC, *et al.*** Elucidating the rimosamide-detoxin natural product families and their biosynthesis using metabolite/gene cluster correlations. ACS Chem Biol 2016;11:3452-3460.

34. **Stintzi A, Johnson Z, Stonehouse M, Ochsner U, Meyer JM, *et al.*** The pvc gene cluster of *Pseudomonas aeruginosa*: role in synthesis of the pyoverdine chromophore and regulation by PtxR and PvdS. J Bacteriol 1999;181:4118-4124.

35. **Stintzi A, Cornelis P, Hohnadel D, Meyer JM, Dean C, *et al.*** Novel pyoverdine biosynthesis gene(s) of *Pseudomonas aeruginosa* PAO. Microbiology 1996;142:1181-1190.

36. **Chen XH, Koumoutsi A, Scholz R, Eisenreich A, Schneider K, *et al.*** Comparative analysis of the complete genome sequence of the plant growth-promoting bacterium *Bacillus amyloliquefaciens* FZB42. Nat Biotechnol 2007;25:1007-1014.

37. **Koumoutsi A, Chen XH, Henne A, Liesegang H, Hitzeroth G, *et al.*** Structural and functional characterization of gene clusters directing nonribosomal synthesis of bioactive cyclic lipopeptides in *Bacillus amyloliquefaciens* strain FZB42. J Bacteriol 2004;186:1084-1096.

38. **Arakawa K, Sugino F, Kodama K, Ishii T, Kinashi H.** Cyclization mechanism for the synthesis of macrocyclic antibiotic lankacidin in *Streptomyces rochei*. Chem Biol 2005;12:249-256.

39. **Kinashi H, Fujii S, Hatani A, Kurokawa T, Shinkawa H.** Physical mapping of the linear plasmid pSLA2-L and localization of the eryAI and actI homologs. Biosci Biotechnol Biochem 1998;62:1892-1897.

40. **Masanori Suwa, Hiroyuki Sugino, Akiko Sasaoka, Eijiro Mori, Shingo Fujii, *et al.*** Identification of two polyketide synthase gene clusters on the linear plasmid pSLA2-L in *Streptomyces rochei*. Gene 2000;246:123-131.

41. **Hiratsu K, Mochizuki S, Kinashi H.** Cloning and analysis of the replication origin and the telomeres of the large linear plasmid pSLA2-L in *Streptomyces rochei*. Mol Gen Genet 2000;263:1015-1021.

42. **Mochizuki S, Hiratsu K, Suwa M, Ishii T, Sugino F, *et al.*** The large linear plasmid pSLA2-L of *Streptomyces rochei* has an unusually condensed gene organization for secondary metabolism. Mol Microbiol 2003;48:1501-1510.

43. **Koumoutsi A, Chen XH, Henne A, Liesegang H, Hitzeroth G, *et al*.** Structural and functional characterization of gene clusters directing nonribosomal synthesis of bioactive cyclic lipopeptides in *Bacillus amyloliquefaciens* strain FZB42. J Bacteriol 2004;186:1084-1096.

44. **Jenul C, Sieber S, Daeppen C, Mathew A, Lardi M, *et al.*** Biosynthesis of fragin is controlled by a novel quorum sensing signal. Nat Commun 2018;9:1297.

45. **Satria A Kautsar, Kai Blin, Simon Shaw, Jorge C Navarro-Muñoz, Barbara R Terlouw, *et al.*** MIBiG 2.0: A repository for biosynthetic gene clusters of known function. Nucleic Acids Res 2020;48:D454-D458.

471 46. **Ali S, Duan J, Charles TC, Glick BR.** A bioinformatics approach to the determination
472 of genes involved in endophytic behavior in *Burkholderia* spp. J Theor Biol 2014;343:193-
473 198.
474 47. **Jahn L, Hofmann U, Ludwig-Müller J.** Indole-3-acetic acid is synthesized by the
475 endophyte *Cyanodermella asteris* via a tryptophan-dependent and - independent way and
476 mediates the interaction with a non-host plant. Int J Mol Sci 2021;22:2651.
477 48. **Oteino N, Lally RD, Kiwanuka S, Lloyd A, Ryan D, *et al.*** Plant growth promotion
478 induced by phosphate solubilizing endophytic *Pseudomonas isolates.* Front Microbiol
479 2015;6:745.
480 49. **Taghavi S, Garafola C, Monchy S, Newman L, Hoffman A, *et al.*** Genome survey
481 and characterization of endophytic bacteria exhibiting a beneficial effect on growth and
482 development of poplar trees. Appl Environ Microbiol 2009;75:748-757
483 50. **Cueva-Yesquén LG, Goulart MC, Attili de Angelis D, Nopper Alves M, Fantinatti-**
484 **Garboggini F.** Multiple plant growth-promotion traits in endophytic bacteria retrieved in the
485 vegetative stage from passionflower. Front Plant Sci 2021;11:621740.
486 51. **Jiménez-Gómez A, García-Estévez I, Escribano-Bailón MT, García-Fraile P,**
487 **Rivas R.** Bacterial fertilizers based on *Rhizobium laguerreae* and *Bacillus halotolerans*
488 enhance cichorium endivia L. Phenolic compound and mineral contents and plant development.
489 Foods 2021;10:424.
490 52. **King E, Ward MK, Raney DE.** Two simple media for the demonstration of pyocyanin
491 and fluorescin. *J Lab Clin Med* 1954;44:301–307.
492 53. **Miller LT.** Single derivatization method for routine analysis of bacterial whole-cell
493 fatty acid methyl esters, including hydroxy acids. J Clin Microbiol 1982;16:584-586.

494 54. **Kuykendall L D, Roy M A, O'Neill J J, Devine T E.** Fatty acids, antibiotic resistance,
495 and deoxyribonucleic acid homology groups of *Bradyrhizobiurn japonicum*. Int J Syst
496 Bacteriol 1988;38:358–361.
497 55. **Moss CW, Lambert-Fair MA.** Location of double bonds in monounsaturated fatty
498 acids of *Campylobacter cryaerophila* with dimethyl disulfide derivatives and combined gas
499 chromatography-mass spectrometry. J Clin Microbiol 1989;27:1467-1470.
500 56. **Yu QT, Liu BN, Zhang JY, Huang ZH**. Location of methyl branchings in fatty acids:
501 fatty acids in uropygial secretion of Shanghai duck by GC-MS of 4,4-dimethyloxazoline
502 derivatives. Lipids 1988;23:804-10.
503 57. **Spitzer V.** Structure analysis of fatty acids by gas chromatography--low resolution
504 electron impact mass spectrometry of their 4,4-dimethyloxazoline derivatives--a review. Prog
505 Lipid Res 1996;35:387-408.
506 58. **Harvey DJ.** Picolinyl esters as derivatives for the structural determination of long chain
507 branched and unsaturated fatty acids. Biomedical Mass Spectrometry 1982;9:33–38.
508 59. **Palleroni NJ (2005).** Genus I. Pseudomonas Migula 1894, 237AL (nom. cons., Opin.
509 5 of the Jud. Comm. 1952, 121). In Bergey's Manual of Systematic Bacteriology, 2nd edn..,
510 vol. 2B, pp. 323–379. Edited by Boone DR, Brenner DJ, Castenholz RW, Garrity GM, Krieg
511 NR, Staley JT. New York: Springer
512 60. **Chang DH, Rhee MS, Kim JS, Lee Y, Park MY, Kim H, *et al.*** *Pseudomonas*
513 *kribbensis* sp. nov., isolated from garden soils in Daejeon, Korea. Antonie Van Leeuwenhoek
514 2016;109:1433-1446.
515 61. **Jia J, Wang X, Deng P, Ma L, Baird SM, *et al.*** *Pseudomonas glycinae* sp. nov.
516 isolated from the soybean rhizosphere. Microbiology open 2020;9:e1101.
517 62. **Bligh EG, Dyer WJ.** A rapid method of total lipid extraction and purification. Can J
518 Biochem Physiol 1959;37:911-917.

519 63. **Tindall BJ, Sikorski J, Smibert RA, Krieg NR (2017).** Phenotypic Characterization
520 and the Principles of Comparative Systematics. In: Methods for General and Molecular
521 Microbiology. John Wiley & Sons, Ltd. pp. 330–393.
522 64. **Kwon SW, Kim JS, Park IC, Yoon SH, Park DH, *et al.*** *Pseudomonas koreensis* sp.
523 nov., *Pseudomonas umsongensis* sp. nov. and *Pseudomonas jinjuensis* sp. nov., novel species
524 from farm soils in Korea. Int J Syst Evol Microbiol 2003;53:21-27.

525 **Figure legends**

526 **Fig. 1.** Multilocus sequence analysis (MLSA) phylogenetic tree based on the 16S rRNA, *rpoB*,
527 *gyrB*, and *rpoD* concatenated sequences with an average length of 9,791 nucleotides showing
528 the position of strain FIT81^T among related species. Sequences were aligned by MUSCL
529 algorithm, and the phylogenetic tree was constructed with MEGA 7 software by using
530 Maximum Likelihood statistical method, Jukes-Cantor substitution method, and pairwise
531 deletion for the missing data. Bootstrap values >50% based on 1000 replications are indicated
532 on branches. Bar, 1 nt substitution per 100 nt.

533 **Fig. 2.** Strain FIT81^T Genome Blast Distance Phylogeny (GBDP) phylogenetic tree based on
534 genome data retrieved from the TYGS server. Branch lengths were calculated with formula D5
535 and the algorithm of greedy with trimming. Pseudo-bootstrap values >60% based on 100
536 replications are indicated on branches. Bar, 1 nt substitution per 100 nt.

537 **Fig. 3.** Strain FIT81^T uranyl acetate negative stain and image captured by transmission electron
538 microscopy (TEM).

539 **Fig. 4.** Two-dimensional thin-layer chromatography (TLC) of the polar lipids fraction of strain
540 FIT81^T. The position of phosphatidylethanolamine (PE), diphosphatidylglycerol (DPG),
541 phosphatidylglycerol (PG), glycolipid (GL), phospholipid (PL), and aminolipid (AL) is
542 indicated by arrows.

543 **Table 1.** Genome-to-genome computational relatedness of the top-five strain FIT81^{T} closest related species.

Species	**Genome size (bp)**	**GC (%)**	**original ANI (%)**	**ortho ANI (%)**	**ANIu (%)**	**ANIb and [% aligned nucleotides]**	**ANIm and [% aligned nucleotides]**	**dDDH and [% model CI]**
strain FIT81^{T}	6.492.796	60.6	-	-	-	-	-	-
P. gozinkensis IzPS32d^{T}	6.563.527	60.3	93.6	94.3	94.0	93.7 [83.2]	94.5 [84.8]	56.1% [53.4 - 58.8%]
P. glycinae MS586^{T}	6.396.728	60.5	93.6	94.0	93.8	93.2 [82.5]	94.4 [82.3]	54.9% [52.1 - 57.6%]
P. allokribbensis IzPS23^{T}	6.565.027	60.3	91.0	91.5	91.5	90.9 [82.5]	91.9 [82.6]	44.4% [41.9 - 47.0%]
'*P. kribbensis*' 46-2	6.324.282	60.5	90.9	91.3	91.3	90.7 [81.5]	91.8 [81.3]	43.9% [41.4 - 46.5%]
P. koreensis PS9-14^{T}	6.123.913	60.5	87.5	87.9	87.5	86.9 [72.3]	89.0 [71.7]	34.7% [32.2 - 37.2%]

544

545 **Table 2.** Main cellular fatty acids detected as FAMEs in strain FIT81^T and the closest related
546 species. Strains: 1, strain FIT81^T; 2, *P. gozinkensis* IzPS32d^T [20]; 3, *P. glycinae* MS586^T [61];
547 4, *P. allokribbensis* IzPS23^T [20]; 5, '*P. kribbensis*' 46-2 [60], and 6, *P. koreensis* Ps9-14^T [64].
548 Data for FIT81^T were obtained in this study whereas for other species were extracted from

Fatty acid	**1**	**2**	**3**	**4**	**5**	**6**
$C_{10:0}$	TR	ND	TR	ND	ND	ND
$C_{10:0}$ 3-OH	4.1	4.2	6.6	4.1	5.4	2.2
$C_{12:0}$ 2-OH	3.9	4.9	5.5	5.1	6.8	5.0
$C_{12:0}$ 3-OH	4.4	5.0	6.7	5.4	7.5	4.0
$C_{12:1}$ 3-OH	TR	ND	ND	ND	ND	ND
$C_{12:0}$	3.7	2	2.9	1.8	ND	TR
$C_{14:0}$	TR	TR	TR	TR	1.2	ND
$C_{16:0}$	30.6	32.4	22.9	31.9	33.4	33
$C_{17:0}$ cyclo	3.8	17.7	10.3	16.1	15.1	2.0
$C_{18:1}$ ω7c	14.4	ND	ND	ND	ND	ND
$C_{18:0}$	1.5	TR	TR	TR	1.6	TR
Summed feature 3 ($C_{16:1}$ ω7c/$C_{15:0}$ iso 2-OH)	30.3	18.3	23.6	19.8	16.8	37

549 literature.

550

551 **Table 3.** Biochemical features of strain FIT81^T and its related species.

552 Strains: 1, strain FIT81^T; 2, *P. gozinkensis* IzPS32d^T; 3, *P. glycinae* MS586^T; 4, *P.*
553 *allokribbensis* IzPS23^T; 5, '*P. kribbensis*' 46-2, and 6, *P. koreensis* Ps9-14^T. Data for FIT81^T,
554 *P. glycinae* MS586^T (= LMG 30275^T), and '*P. kribbensis*' 46-2 (= DSM 100278^T) were
555 obtained in this study whereas those for *P. gozinkensis* IzPS32d^T, *P. allokribbensis* IzPS23^T,
556 and *P. koreensis* Ps9-14^T were extracted from literature [20, 64]. Symbols legend are positive
557 (+), negative (-), weak or uncertain (w), variability in literature (-/+), and not determined (ND).

Characteristics	**1**	**2**	**3**	**4**	**5**	**6**
Fluorescence (fluorescein pigment)	+	+	+	+	-	+
Growth at 37ºC	-	-	-	-	-	-/+
Growth on 4% NaCl	+	+	+	+	+	+
Carbon source utilization:						
D-Arabitol	+	-	+	-	+	+
D-Aspartic acid	-	-	-	-	w	+
D-Serine	-	+	+	-	w	ND
α-D-Glucose	+	+	+	+	+	+
D-Fructose-6-phosphate	w	-	w	-	+	ND
N-Acetyl-D-glucosamine	+	-	+	-	+	+
D-Galactose	+	w	+	w	+	+
Pectin	w	-	w	-	w	ND
Citrate	+	+	+	+	+	+
D-Fucose	w	-	w	-	+	ND
D-Mannose	+	+	+	+	+	+
Inosine	+	-	+	-	+	+
D-Galacturonic acid	w	-	w	-	+	-/+
L-Arabinose	+	+	+	+	+	+
Glycerol	+	+	+	ND	+	+
L-Galactonic acid lactone	w	-	w	-	+	+
D-Glucuronic acid	w	-	w	-	+	-/+
Glucuronamide	+	-	+	-	+	+
D-Malic acid	+	-	w	-	+	ND
Mucic acid	+	+	+	w	+	ND
Bromo-succinic acid	+	-	+	-	+	ND
α-Keto-butyric acid	w	-	w	-	w	-/+
Acetoacetic acid	w	-	w	-	w	ND
Quinic acid	+	+	+	+	+	+

D-Saccharic acid	+	+	+	-	+	+
Tween 40	+	w	+	-	+	+
Enzymatic activity						
Alkaline phosphatase	+	+	+	+	+	ND
C4 esterase	+	+	+	+	+	ND
C8 esterase lipase	+	+	+	+	+	ND
C14 lipase	+	ND	+	ND	+	ND
Leucin arylamidase	w	+	+	+	w	ND
Valine arylamidase	w	+	+	+	w	ND
Cystine arylamidase	w	ND	w	ND	w	ND
Trypsin	+	ND	+	ND	+	ND
α-Chymotrypsin	w	ND	w	ND	w	ND
Acid phosphatase	+	+	+	+	+	ND
Naphthol-AS-BI-phosphohydrolase	+	+	+	+	+	ND
Lysine decarboxylase	-	ND	-	ND	+	ND
Arginine dihydrolase	+	ND	+	ND	+	+
Ornithine decarboxylase	-	ND	-	ND	-	ND
Gelatin hydrolysis (protease)	+	ND	+	ND	+	+
Urease	+	ND	+	ND	+	ND
Esculin hydrolysis (β-glucosidase)	+	ND	+	ND	+	ND
β-Galactosidase (p-nitrophenyl-β-D-galactopyranosidase)	-	ND	-	ND	-	ND

558

Pseudomonas fitomaticsae sp. nov., isolated at Marimurtra Botanical Garden in Blanes, Catalonia-Spain

Kostadin Evgeniev Atanasov[1,2], David Miñana Galbis[3], Deborah Cornadó[4], Annabel Serpico[4], Guiomar Sánchez[4], Montserrat Bosch[4], Albert Ferrer[1,5] and Teresa Altabella[1,2]

[1]Center for Research in Agricultural Genomics (CSIC-IRTA-UAB-UB), Bellaterra, Barcelona, Spain.

[2]Department of Biology, Healthcare and the Environment, Plant Physiology Section, Faculty of Pharmacy and Food Sciences, Universitat de Barcelona, Spain.

[3]Department of Biology, Healthcare and the Environment, Microbiology Section, Faculty of Pharmacy and Food Sciences, Universitat de Barcelona, Spain.

[4]Applied Microbiology and Biotechnology Unit, LEITAT Technological Center, Terrassa, Spain.

[5]Department of Biochemistry and Physiology, Faculty of Pharmacy and Food Sciences, Universitat de Barcelona, Spain.

Corresponding author: Kostadin E. Atanasov

The email address for the corresponding author: evgenievatanassov@ub.edu

List of Supplemental Figures and Tables

Supplemental Figure 1 (Fig. S1): Phylogenetic tree constructed on the 1,453 average 16S rRNA sequences length of the strain FIT81^T relatives. Sequence alignment was performed by using MUSCL algorithm and tree constructed by the statistical method of Maximum Likelihood, Jukes-Cantor substitution method, and pairwise deletion of gaps or missing data. Bootstrap test of phylogeny was performed with 1000 replications and values >50% indicated on branches. Bar, 1 nt substitution per 100 nt.

Supplemental Table 1 (Table S1): Species, strain designation, accession ID, and sequence identity for the 16S rRNA nucleotide sequence blast analysis of strain FIT81^T and its closest relative species.

Supplemental Table 2 (Table S2): Species, strain designation, assembly ID, and sequence identity for the MLSA nucleotide blast of strain FIT81^T and its closest relative species.

Supplemental Table 3 (Table S3): Genome mining of strain FIT81^T, *P. gozinkensis* IzPS32d^T; 3, *P. glycinae* MS586^T.

Supplemental Table 4 (Table S4): Identification of endophytic behavior genes: 1, strain FIT81^T; 2, *P. gozinkensis* IzPS32d^T; 3, *P. glycinae* MS586^T.

Fig. S1

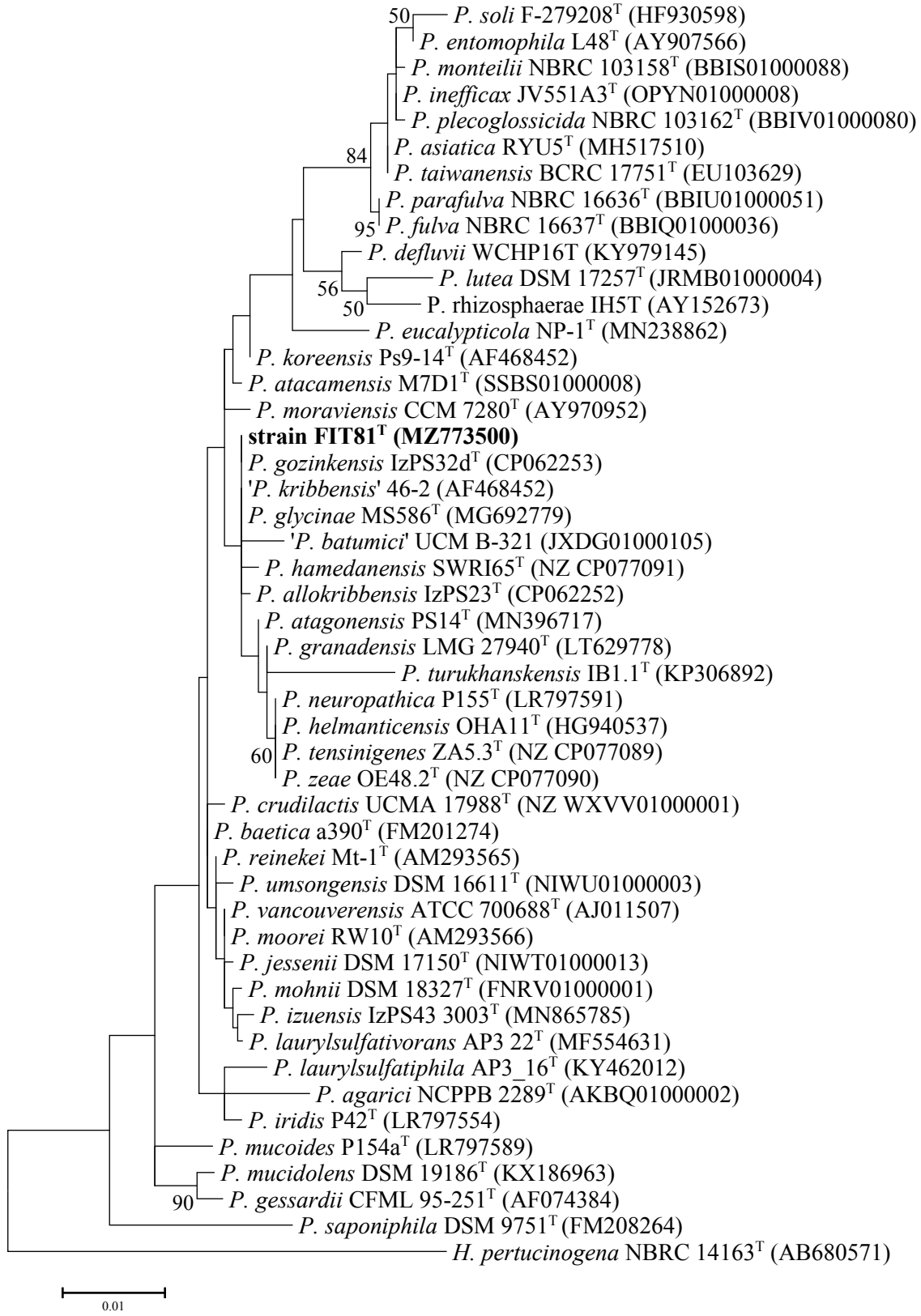
50
P. soli F-279208T (HF930598)
P. entomophila L48T (AY907566)
P. monteilii NBRC 103158T (BBIS01000088)
P. inefficax JV551A3T (OPYN01000008)
P. plecoglossicida NBRC 103162T (BBIV01000080)
84
P. asiatica RYU5T (MH517510)
P. taiwanensis BCRC 17751T (EU103629)
P. parafulva NBRC 16636T (BBIU01000051)
95
P. fulva NBRC 16637T (BBIQ01000036)
P. defluvii WCHP16T (KY979145)
56
P. lutea DSM 17257T (JRMB01000004)
50
P. rhizosphaerae IH5T (AY152673)
P. eucalypticola NP-1T (MN238862)
P. koreensis Ps9-14T (AF468452)
P. atacamensis M7D1T (SSBS01000008)
P. moraviensis CCM 7280T (AY970952)
strain FIT81T (MZ773500)
P. gozinkensis IzPS32dT (CP062253)
'P. kribbensis' 46-2 (AF468452)
P. glycinae MS586T (MG692779)
'P. batumici' UCM B-321 (JXDG01000105)
P. hamedanensis SWRI65T (NZ CP077091)
P. allokribbensis IzPS23T (CP062252)
P. atagonensis PS14T (MN396717)
P. granadensis LMG 27940T (LT629778)
P. turukhanskensis IB1.1T (KP306892)
P. neuropathica P155T (LR797591)
P. helmanticensis OHA11T (HG940537)
60
P. tensinigenes ZA5.3T (NZ CP077089)
P. zeae OE48.2T (NZ CP077090)
P. crudilactis UCMA 17988T (NZ WXVV01000001)
P. baetica a390T (FM201274)
P. reinekei Mt-1T (AM293565)
P. umsongensis DSM 16611T (NIWU01000003)
P. vancouverensis ATCC 700688T (AJ011507)
P. moorei RW10T (AM293566)
P. jessenii DSM 17150T (NIWT01000013)
P. mohnii DSM 18327T (FNRV01000001)
P. izuensis IzPS43 3003T (MN865785)
P. laurylsulfativorans AP3 22T (MF554631)
P. laurylsulfatiphila AP3_16T (KY462012)
P. agarici NCPPB 2289T (AKBQ01000002)
P. iridis P42T (LR797554)
P. mucoides P154aT (LR797589)
P. mucidolens DSM 19186T (KX186963)
90
P. gessardii CFML 95-251T (AF074384)
P. saponiphila DSM 9751T (FM208264)
H. pertucinogena NBRC 14163T (AB680571)
0.01

Table S1

Species	Strain	Accession ID	Identity	Cover	Length	E value
'*P. kribbensis*'	46-2	AF468452	99.9%	95%	1459	0.0
P. gozinkensis	IzPS32d^{T}	CP062253	99.9%	100%	1533	0.0
P. glycinae	MS586^{T}	MG692779	99.9%	95%	1459	0.0
P. allokribbensis	IzPS23^{T}	CP062252	99.8%	100%	1533	0.0
P. atacamensis	M7D1^{T}	SSBS01000008	99.7%	95%	1459	0.0
P. moraviensis	CCM 7280^{T}	AY970952	99.6%	95%	1459	0.0
P. granadensis	LMG 27940^{T}	LT629778	99.6%	95%	1459	0.0
P. koreensis	Ps9-14^{T}	AF468452	99.6%	94%	1455	0.0
P. reinekei	Mt-1^{T}	AM293565	99.4%	95%	1459	0.0
P. hamedanensis	SWRI65^{T}	CP077091	99.4%	100%	1542	0.0
P. vancouverensis	ATCC 700688^{T}	AJ011507	99.3%	95%	1459	0.0
P. jessenii	DSM 17150^{T}	NIWT01000013	99.3%	95%	1459	0.0
P. baetica	a390^{T}	FM201274	99.2%	94%	1446	0.0
P. neuropathica	P155^{T}	LR797591	99.2%	80%	1232	0.0
P. atagonensis	PS14^{T}	MN396717	99.2%	95%	1460	0.0
P. izuensis	IzPS43_3003^{T}	MN865785	99.1%	95%	1459	0.0
'*P. batumici*'	UCM B-321	JXDG01000105	99.1%	95%	1459	0.0
P. zeae	OE48.2^{T}	CP077090	99.0%	100%	1542	0.0
P. tensinigenes	ZA5.3^{T}	CP077089	99.0%	100%	1542	0.0
P. helmanticensis	OHA11^{T}	HG940537	99.0%	95%	1459	0.0
P. crudilactis	UCMA 17988^{T}	WXVV01000001	99.0%	99%	1525	0.0
P. laurylsulfativorans	AP3_22^{T}	MF554631	98.8%	95%	1459	0.0

P. umsongensis	DSM 16611^T	NIWU01000003	98.8%	95%	1459	0.0
P. mohnii	DSM 18327^T	FNRV01000001	98.6%	95%	1459	0.0
P. parafulva	NBRC 16636^T	BBIU01000051	98.6%	95%	1459	0.0
P. mucoides	P154a^T	LR797589	98.6%	80%	1232	0.0
P. fulva	NBRC 16637^T	BBIQ01000036	98.6%	95%	1459	0.0
P. iridis	P42^T	LR797554	98.5%	80%	1232	0.0
P. laurylsulfatiphila	AP3_16^T	KY462012	98.5%	95%	1460	0.0
P. lutea	DSM 17257^T	JRMB01000004	98.4%	95%	1459	0.0
P. defluvii	WCHP16^T	KY979145	98.3%	95%	1459	0.0
P. asiatica	RYU5^T	MH517510	98.3%	95%	1459	0.0
P. taiwanensis	BCRC 17751^T	EU103629	98.3%	94%	1451	0.0
P. eucalypticola	NP-1^T	MN238862	98.3%	92%	1423	0.0
P. soli	F-279,208^T	HF930598	98.2%	92%	1421	0.0
P. turukhanskensis	IB1.1^T	KP306892	98.2%	92%	1412	0.0
P. gessardii	CFML 95-251^T	AF074384	98.2%	95%	1459	0.0
P. mucidolens	DSM 19186^T	KX186963	98.2%	95%	1459	0.0
P. inefficax	JV551A3^T	OPYN01000008	98.2%	95%	1459	0.0
P. agarici	NCPPB 2289^T	AKBQ01000002	98.2%	95%	1459	0.0
P. rhizosphaerae	IH5^T	AY152673	98.2%	95%	1459	0.0
P. plecoglossicida	NBRC 103162^T	BBIV01000080	98.15%	95%	1459	0.0
P. monteilii	NBRC 103158^T	BBIS01000088	98.2%	95%	1459	0.0
P. moorei	RW10^T	AM293566	98.1%	95%	1459	0.0
P. entomophila	L48^T	AY907566	98.1%	95%	1459	0.0
P. saponiphila	DSM 9751^T	(FM208264)	96.5%	99%	1530	0.0

H. pertucinogena	NBRC 14163^{T}	(AB680571)	94.5%	95%	1459	0.0

Table S2

Species	**Strain**	Accession ID	**Identity**	**Cover**	**Length**	**E value**
P. gozinkensis	IzPS32d^{T}	NZ_CP062253	98.2	99%	9873	0.0
P. glycinae	MS586^{T}	NZ_CP014205	98.2	100%	9799	0.0
'*P. kribbensis*'	46-2	NZ_CP029608	97.9	99%	9799	0.0
P. allokribbensis	IzPS23^{T}	NZ_CP062252	97.40	100%	9873	0.0
P. koreensis	Ps9-14^{T}	NZ_JAAQYM010000010	97.0	99%	9795	0.0
P. atagonensis	PS14^{T}	NZ_VXCA010000019	96.9	100%	9797	0.0
P. atacamensis	M7D1^{T}	NZ_SSBS01000010	96.5	100%	9799	0.0
P. moraviensis	CCM 7280^{T}	NZ_LT629788	96.4	100%	9799	0.0
P. granadensis	LMG 27940^{T}	NZ_LT629778	96.3	100%	9799	0.0
P. baetica	a390^{T}	NZ_PHHE01000001	96.1	99%	9786	0.0
P. crudilactis	UCMA 17988^{T}	NZ_WXVV01000001	96.1	100%	9865	0.0
P. zeae	OE48.2^{T}	NZ_CP077090	96.0	100%	9879	0.0
P. tensinigenes	ZA 5.3^{T}	NZ_CP077089	96.0	100%	9879	0.0
P. neuropathica	P155^{T}	NZ_JACOPX010000000	95.9	97%	9569	0.0
P. helmanticensis	OHA11^{T}	SAMN04488483	95.9	100%	9796	0.0
P. hamedanensis	SWRI65^{T}	NZ_CP012001	95.6	100%	9879	0.0
P. izuensis	IzPS43_3003^{T}	NZ_WTFT01000001	94.9	100%	9799	0.0
P. vancouverensis	ATCC 700688^{T}	NZ_RRZK01000005	94.9	99%	9799	0.0
P. jessenii	DSM 17150^{T}	NZ_FNTC01000002	94.8	100%	9799	0.0
P. umsongensis	DSM 16611^{T}	NZ_LT629767	94.7	100%	9799	0.0
P. laurylsulfatiphila	AP3_16^{T}	NZ_NIRS01000001	94.7	99%	9800	0.0
P. laurylsulfativorans	AP3_22^{T}	NZ_MUJK01000010	94.7	98%	9642	0.0

P. iridis	P42^{T}	NZ_JACOPU010000001	94.5	97%	9572	0.0
P. reinekei	Mt-1^{T}	NZ_LT629709	94.4	100%	9799	0.0
P. moorei	RW10^{T}	NZ_FNKJ01000003	94.2	100%	9799	0.0
P. mohnii	DSM 18327^{T}	NZ_FNRV01000002	94.2	100%	9799	0.0
P. mucoides	P154a^{T}	NZ_JACOPW010000001	93.6	97%	9572	0.0
'*P. batumici*'	UCM B-321	NZ_JXDG01000001	93.6	100%	9799	0.0
P. gessardii	CFML 95-251^{T}	NZ_FNKR01000003	93.0	100%	9802	0.0
P. saponiphila	DSM 9751^{T}	NZ_FNTJ00000000	92.6	99%	9870	0.0
P. mucidolens	DSM 19186^{T}	NZ_LS483433	92.5	100%	9799	0.0
P. agarici	NCPPB 2289^{T}	NZ_FOAR01000077	91.4	99%	9799	0.0
P. eucalypticola	NP-1^{T}	NZ_CP056030	90.1	99%	9763	0.0
P. rhizosphaerae	IH5^{T}	NZ_CP009533	89.3	99%	9796	0.0
P. plecoglossicida	NBRC 103162^{T}	NZ_BBIV01000097	89.2	100%	9805	0.0
P. entomophila	L48^{T}	CT573326	89.1	99%	9805	0.0
P. lutea	DSM 17257^{T}	JRMB01000001	88.9	99%	9793	0.0
P. inefficax	JV551A3^{T}	NZ_OPYN01000001	88.9	100%	9805	0.0
P. asiatica	RYU5^{T}	NZ_BLJF01000001	88.9	100%	9805	0.0
P. monteilii	NBRC 103158^{T}	NZ_BBIS01000132	88.8	100%	9805	0.0
P. soli	F-279,208^{T}	NZ_CP009365	88.7	99%	9767	0.0
P. taiwanensis	BCRC 17751^{T}	NZ_KE384450	88.7	100%	9797	0.0
P. parafulva	NBRC 16636^{T}	NZ_BBIU01000055 - NZ_BBIU01000000	88.3	100%	9802	0.0
P. fulva	NBRC 16637^{T}	LAWW01000001	88.0	100%	9802	0.0
H. pertucinogena	JCM 11590^{T}	NZ_BMNN00000000	84.1	86%	9814	0.0

Table S3

	Region	Type of metabolite	Position	Most similar known cluster	Cluster similarity	MIBiG comparison
strain FIT81^T	**1**	Arylpolyene	675,175 - 718,779	APE Vf	40%	Fragin (*Burkholderia cenocepacia* H111) Fellutamide B (*Aspergillus nidulans* FGSC A4) Showdomycin (*Streptomyces showdoensis*)
	2	RiPP-like	1,652,937 - 1,661,494	-	0	Duramycin (Streptomyces cinnamoneus) Butyrivibriocin AR10 (*Butyrivibrio fibrisolvens*) Citrulassin E (*Streptomyces glaucescens*)
	3	NRPS Terpene	2,318,719 - 2,394,454	Pyoverdin	20%	Sodorifen (*Serratia plymuthica* 4Rx13) 2-methylisoborneol (*Pseudanabaena* sp. dqh15) 2-methylisoborneol (*Streptomyces griseus* subsp. *griseus* NBRC 13350)
	4	RiPP-like	2,686,928 - 2,697,767	-	0	Lipopolysaccharide (*Xanthomonas campestris* pv. *campestris*) T3 toxin (*Cylindrospermopsis raciborskii* T3) Saxitoxin (*Cylindrospermopsis raciborskii* T3)

5	NRPS	2,811,220 - 2,886,660	Lokisin	71%	Gacamide A (*Pseudomonas fluorescens* Pf0-1) Bananamide (*Pseudomonas fluorescens*) Anikasin (*Pseudomonas fluorescens*)
6	NRPS	2,893,410 -2,952,691	Rimosamide	28%	Massetolide A (*Pseudomonas fluorescens* SS101) Thalassospiramide A (*Tistrella bauzanensis*) Sevadicin (*Paenibacillus larvae*)
7	Siderophore	3,443,252 - 3,462,180	-	0%	Aerobactin (*Xenorhabdus szentirmaii* DSM 16338) Aerobactin (*Pantoea ananatis*) Ochrobactin (*Ochrobactrum anthropi*) Desferrioxamine (*Pantoea agglomerans*)
8	Betalactone	4,195,007 - 4,218,271	Fengycin	13%	Jadomycin (*Streptomyces venezuelae* ATCC 10712) Cepacin A (*Burkholderia ambifaria* IOP40-10) Bromopyrroles/bromophenols (*Marinomonas mediterranea* MMB-1)
9	Ranthipeptide	4,480,897 - 4,502,327	Pyoverdin	11%	Erythreapeptin (*Saccharopolyspora erythraea* NRRL 2338) Bicereucin (*Bacillus cereus* SJ1) FR-900098 (*Streptomyces rubellomurinus*)

	10	NRPS	4,531,025 - 4,584,023	Pyoverdin	21%	Erythrochelin (*Saccharopolyspora erythraea* NRRL 2338) Anabaenopeptin NZ857/nostamide A (*Nostoc punctiforme* PCC 73102) monobactam (*Agrobacterium tumefaciens*)
	11	NAGGN	4,768,261 - 4,783,034	-	0%	Tabtoxin (*Pseudomonas syringae*) Bacilysin (*Bacillus sp*. CS93) 4-hydroxy-3-nitrosobenzamide (*Streptomyces murayamaensis*)
	12	Redox-cofactor	6,092,219 - 6,114,387	Lankacidin C	13%	Prodigiosin (*Serratia sp*.) Prodigiosin (*Serratia marcescens*) Prodigiosin (*Hahella chejuensis* KCTC 2396)
P. gozinkensis IzPS32d^T	**1**	NRPS-like	130.089 - 159.699	Fragin	37%	Fragin (*Burkholderia cenocepacia* H111) Livipeptin (*Streptomyces lividans* 1326) Aspergillic acid (*Aspergillus flavus* NRRL3357)
	2	Arylpolyene	488,336 - 531,964	APE Vf	40%	Aryl polyene (*Escherichia coli* CFT073) Aryl polyene (*Xenorhabdus doucetiae*) Caboxamycin (*Streptomyces sp.* NTK 937)
	3	RiPP-like	1,472,919 - 1,481,478	-	0%	Duramycin (*Streptomyces cinnamoneus*)

					Butyrivibriocin AR10 (*Butyrivibrio fibrisolvens*) Citrulassin E (*Streptomyces glaucescens*)
4	NRPS-like NRPS	2,103,351 - 2,187,903	Pyoverdin	20%	Livipeptin (*Streptomyces lividans* 1326) Fragin (*Burkholderia cenocepacia* H111) Fellutamide B (*Aspergillus nidulans* FGSC A4)
5	RiPP-like	2,415,999 - 2,426,838	-	0%	Lipopolysaccharide (*Xanthomonas campestris* pv. *campestris*) T3 toxin (*Cylindrospermopsis raciborskii* T3) Saxitoxin (Cylindrospermopsis raciborskii T3)
6	NRPS	2,664,065 - 2,733,716	Lokisin	71%	Gacamide A (*Pseudomonas fluorescens* Pf0-1) Bananamide (*Pseudomonas fluorescens*) Anikasin (*Pseudomonas fluorescens*)
7	NRPS	2,741,718 - 2,802,189	Rimosamide	21%	Massetolide A (*Pseudomonas fluorescens* SS101) Thalassospiramide A (*Tistrella bauzanensis*) Sevadicin (*Paenibacillus larvae*)
8	Siderophore	2,847,118 - 2,858,971	-	0%	Ethylenediaminesuccinic acid hydroxyarginine (EDHA) (*Streptomyces avermitilis* MA-4680 = NBRC 14893)

					Lipopolysaccharide (*Xanthomonas campestris* pv. *campestris*) streptonigrin (*Streptomyces flocculus*)
9	Thiopeptide	3,394,589 - 3,424,725	-	0%	Pseudopyronine (*Pseudomonas putida*) Pyrazomycin (*Streptomyces candidus*) Thaxteramide (*Jahnella sp.* MSr9139)
10	Betalactone	4,186,987 - 4,210,223	Fengycin	13%	Jadomycin (*Streptomyces venezuelae* ATCC 10712) Cepacin A (*Burkholderia ambifaria* IOP40-10) Bromopyrroles/bromophenols (*Marinomonas mediterranea* MMB-1)
11	Ranthipeptide	4,485,491 - 4,506,921	Pyoverdin	11%	FR-900098 (*Streptomyces rubellomurinus*) Succinoglycan (*Sinorhizobium meliloti*) Exopolysaccharides (*Burkholderia cenocepacia* J2315)
12	NRPS	4,539,277 - 4,592,278	Pyoverdin	20%	Erythrochelin (*Saccharopolyspora erythraea* NRRL 2338) Anabaenopeptin NZ857/nostamide A (*Nostoc punctiforme* PCC 73102) chloromyxamide (*Myxococcus sp*.)
13	NAGGN	4,747,766 - 4,762,638	-	0%	Tabtoxin (*Pseudomonas syringae*) Bacilysin (*Bacillus sp.* CS93)

						4-hydroxy-3-nitrosobenzamide (*Streptomyces murayamaensis*)
	14	Redox-cofactor	5,936,419 - 5,958,575	Lankacidin C	13%	Prodigiosin (*Serratia sp.*) Prodigiosin (*Serratia marcescens*) Prodigiosin (*Hahella chejuensis* KCTC 2396)
P. glycinae MS586^T	**1**	NAGGN	202,379 - 217,152	-	0%	Tabtoxin (*Pseudomonas syringae*) Bacilysin (*Bacillus sp.* CS93) 4-hydroxy-3-nitrosobenzamide (*Streptomyces murayamaensis*)
	2	NRPS	1,027,109 - 1,078,566	Pyoverdin	20%	Anabaenopeptin NZ857/nostamide A (*Nostoc punctiforme* PCC 73102) Monobactam (*Agrobacterium tumefaciens*) Aspirochlorine (*Aspergillus oryzae* RIB40)
	3	NRPS	2,076,149 - 2,134,645	Rimosamide	28%	Massetolide A (*Pseudomonas fluorescens* SS101) Sevadicin (*Paenibacillus larvae*) Curacomycin (*Streptomyces curacoi*)
	4	NRPS	2,291,136 - 2,358,877	Lokisin	71%	Bananamide (*Pseudomonas fluorescens*)

					Gacamide A (*Pseudomonas fluorescens* Pf0-1) Anikasin (*Pseudomonas fluorescens*)
5	RiPP-like	2,532,324 - 2,541,936	Bacillomycin D	20%	Lipopolysaccharide (*Xanthomonas campestris* pv. *campestris*) alkylresorcinol (*Streptomyces griseus* subsp. *griseus* NBRC 13350) Malleobactin (*Burkholderia thailandensis* E264)
6	Redox-cofactor	2,973,621 - 2,995,777	Lankacidin C	13%	Prodigiosin (*Serratia sp.*) Prodigiosin (*Serratia marcescens*) Prodigiosin (*Hahella chejuensis* KCTC 2396)
7	RiPP-like	4,555,244 - 4,566,131	-	0%	Duramycin (Streptomyces cinnamoneus) butyrivibriocin AR10 (Butyrivibrio fibrisolvens) citrulassin E (Streptomyces Glaucescens)
8	Betalactone	5,098,665 - 5,123,195	Fengycin	13%	Showdomycin (*Streptomyces showdoensis*) Jadomycin (*Streptomyces venezuelae* ATCC 10712) Cepacin A (*Burkholderia ambifaria* IOP40-10)
9	NRPS-like	5,205,531 - 5,235,101	Fragin	37%	Fragin (*Burkholderia cenocepacia* H111) Livipeptin (*Streptomyces lividans* 1326)

					Aspergillic acid (*Aspergillus flavus* NRRL3357)
10	Arylpolyene	5,569,355 - 5,612,983	APE Vf	40%	Aryl polyene (*Escherichia coli* CFT073) Aryl polyene (*Xenorhabdus doucetiae*) Caboxamycin (*Streptomyces sp*. NTK 937
11	NRPS- Terpene	6,231,816 -6,299,285	Pyoverdin	18%	2-methylisoborneol (*Streptomyces griseus* subsp. *griseus* NBRC 13350) Bacilysin (*Bacillus sp*. CS93) Pentostatine/vidarabine (*Streptomyces antibioticus*)

Table S4

		1	2	3
Transport	NAD(P)(+) transhydrogenase (AB-specific)	+	+	+
	Branched-chain amino acid ABC transporter	+	+	+
Secretion and delivery system	Type VI secretion ATPase, ClpV1	+	+	+
Plant polymer degradation/modification	Cupin	+	+	+
	Peptidase M48	+	+	+
Transcriptional regulator	AsnC family transcriptional regulator	+	+	+
	AraC family transcriptional regulator	+	+	+
	Transcriptional regulator, DeoR family	+	+	+
	Transcriptional regulator, LysR family	+	+	+
Detoxification	Glutathione S-transferase	+	+	+
	S-(hydroxymethyl) glutathione dehydrogenase/class III alcohol dehydrogenase	+	+	+
	2-dehydropantoate 2-reductase	+	+	+
	Acetaldehyde dehydrogenase	+	-	-
	Carbonate dehydratase	+	+	+
Redox potential maintenance	Aldehyde dehydrogenase	+	+	+
	L-lactate dehydrogenase	+	+	+
	Malate dehydrogenase	+	+	+
	3-hydroxyisobutyrate dehydrogenase	+	+	+
Plant cell-wall attachment	ndvB	+	+	+
	ndvC	+	+	+
Hormones	1-aminocyclopropane-1-carboxylate deaminase	+	+	+
	indole-3-glycerol phosphate synthase	+	+	+
Phosphate solubilization	pqqA	+	+	+

	pqqB	+	+	+
	pqqC	+	+	+
	pqqD	+	+	+
	pqqE	+	+	+
	pqqF	+	+	+
Other	2-isopropylmalate synthase	+	+	+
	Diaminopimelate decarboxylase	+	+	+

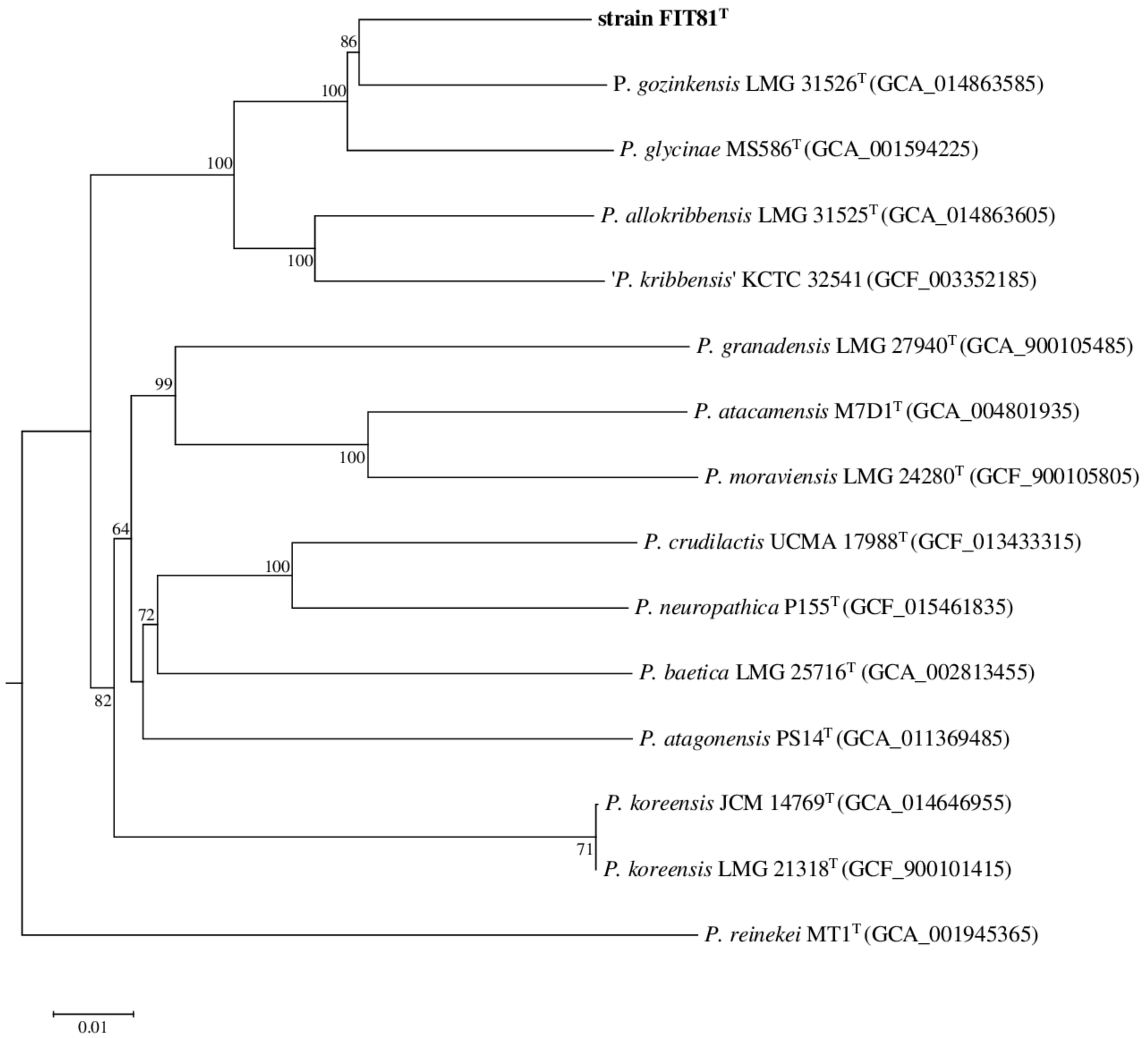
strain FIT81T
86
P. gozinkensis LMG 31526T (GCA_014863585)
100
P. glycinae MS586T (GCA_001594225)
100
P. allokribbensis LMG 31525T (GCA_014863605)
100
'P. kribbensis' KCTC 32541 (GCF_003352185)
P. granadensis LMG 27940T (GCA_900105485)
99
P. atacamensis M7D1T (GCA_004801935)
100
P. moraviensis LMG 24280T (GCF_900105805)
64
P. crudilactis UCMA 17988T (GCF_013433315)
100
P. neuropathica P155T (GCF_015461835)
72
P. baetica LMG 25716T (GCA_002813455)
82
P. atagonensis PS14T (GCA_011369485)
P. koreensis JCM 14769T (GCA_014646955)
71
P. koreensis LMG 21318T (GCF_900101415)
P. reinekei MT1T (GCA_001945365)
0.01

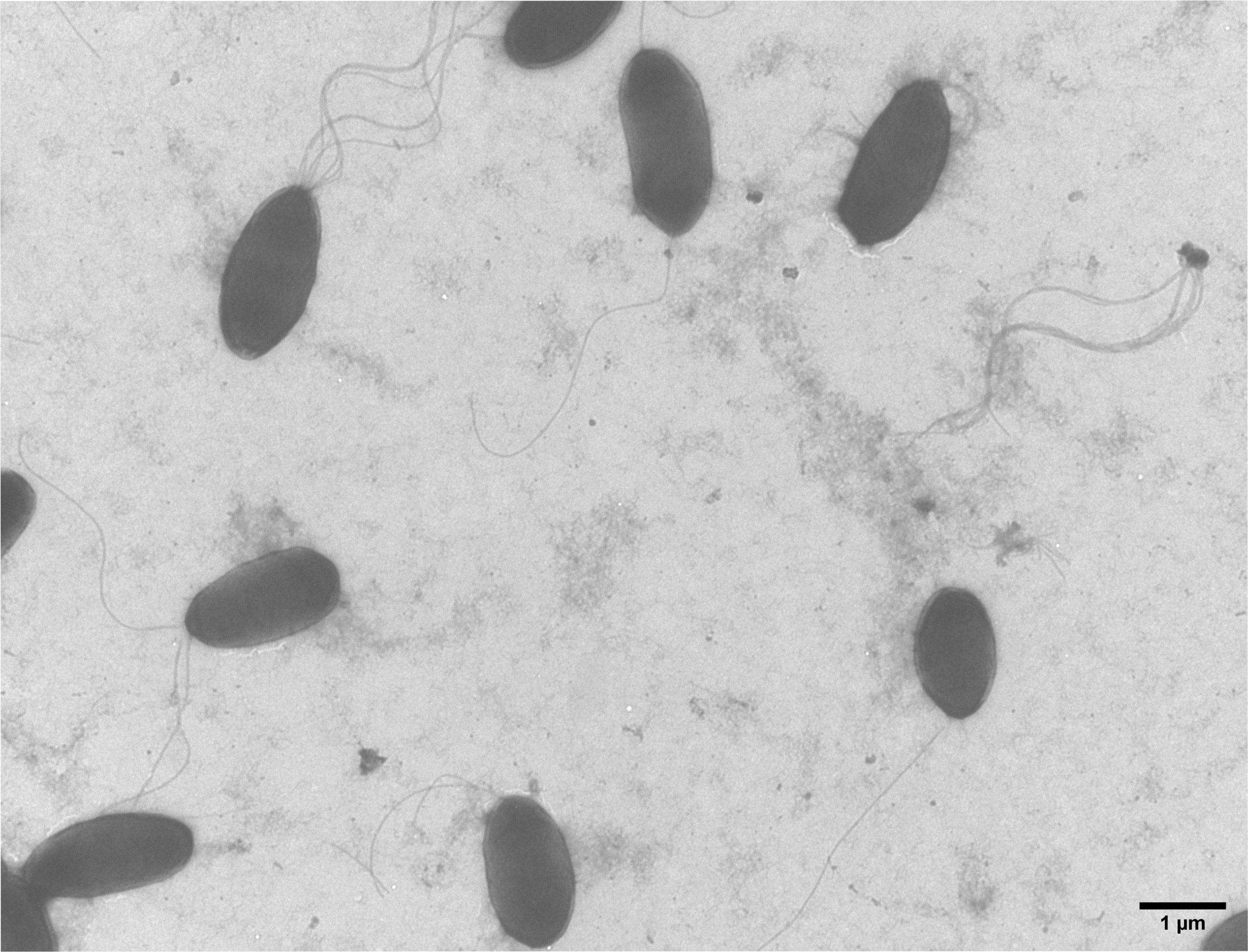
1 µm

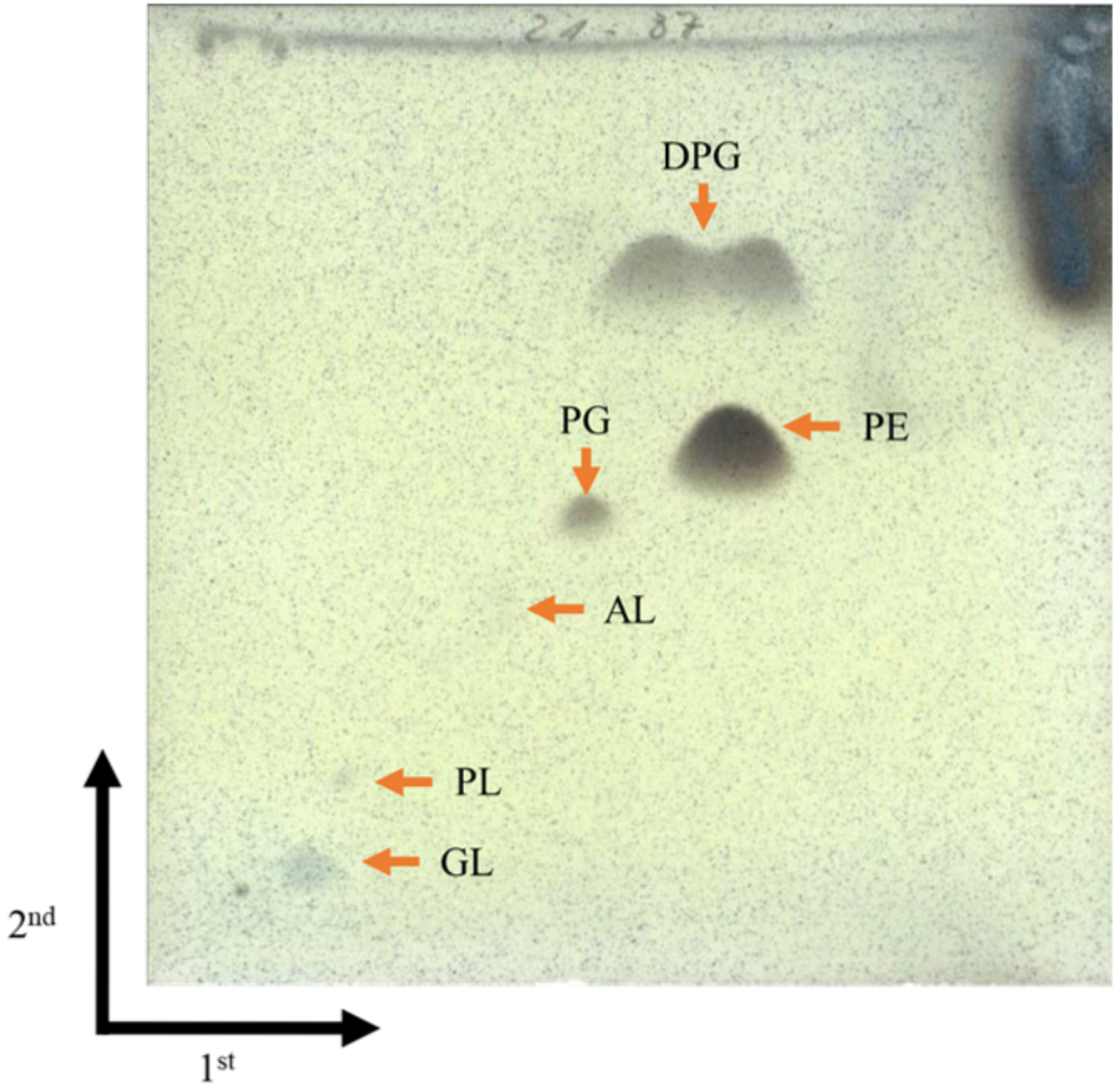
DPG
PG
PE
AL
PL
GL
2nd
1st